Optimizing the Structures of Minimum and Transition State on the Free Energy Surface

Sheng-Yong Yang, Iordan Hristov, Paul Fleurat-Lessard, and Tom Ziegler*

Department of Chemistry, University of Calgary, University Drive 2500, Calgary, Alberta, Canada T2N 1N4

Received: September 8, 2004; In Final Form: October 26, 2004

Presented here is the application of a scheme for optimizing the structures of minima and transition states on the free energy surface (FES) for a path along a fixed reaction coordinate with the aid of ab initio molecular dynamics (AIMD) simulation. In the direction of the reaction coordinate, the values corresponding to the stationary points were optimized using the quasi-Newton method, in which the gradient of the free energy along the reaction coordinate was obtained by a constraint AIMD method, and the Bofill Hessian update scheme was used. The equilibrium values for the other directions were taken as the corresponding averages in the dynamic simulation. This scheme was applied to several elementary bimolecular addition reactions: (A) $BH_3 + H_2O \rightarrow H_2O{\cdot}BH_3$; (B) $BF_3 + NH_3 \rightarrow FB_3{\cdot}NH_3$; (C) $SO_3 + NH_3 \rightarrow O_3S{\cdot}NH_3$; (D) $C_2H_4 + CCl_2 \rightarrow H_4C_2{\cdot}CCl_2$; (E) $Ni(NH_2)_2 + PH_3 \rightarrow (NH_2)_2Ni{\cdot}PH_3$; (F) $W(CO)_5 + CO \rightarrow W(CO)_6$. For reactions A, B, C, and F, no transition state (TS) exists on the potential energy surface (PES). However there is a TS on the FES. This stems from the curvature difference of the PES and $-T\Delta S$ as a function of the reaction coordinate. For all reactions, it is found that the TS shifts toward the complexation product with increasing temperature because of the curvature increase of $-T\Delta S$. The equilibrium bond distances for the inactive coordinates perpendicular to the reaction coordinate always increase with temperature, which is due to the thermal excitation and anharmonicity of the PES.

Introduction

Studies of chemical reactions have traditionally been carried out by locating reactant, transition state, and product structures on the potential energy surface (PES) and connecting them by a minimum energy path. However, recent studies[1−3] have shown that the free energy profile can differ considerably from that of the potential energy surface at 0 K, even when use is made of the same reaction coordinate. Thus, to better understand chemical reactions, one needs to work on the free energy surface (FES). Of special interest is the fact that the position of the transition state along a path characterized by the same reaction coordinate can be quite different at different temperatures.[3] In fact, a transition state present at finite temperatures might be absent on the potential energy surface. Here, we shall study this phenomenon further.

The geometry optimization of stationary points on the PES is by now a routine task.[4] This can be attributed to the fact that the gradient of the potential energy can be readily obtained from quantum mechanical calculations. It is reasonable to assume that, if the gradient of the free energy is available, the same optimization procedure used for the PES could be adopted to carry out optimizations on the FES. Free energy gradients have been evaluated in the past in connection with classical molecular dynamics calculations based on empirical force fields.[5] However, empirical force fields are not suitable for chemical reactions where bonds are formed or broken. Fortunately, bond forming/breaking can be described by ab initio molecular dynamics (AIMD). Especially efficient is the method of Car-Parrinello AIMD (CP-AIMD).[6,7]

In the following, we shall discuss a scheme that evaluates gradients on the FES based on CP-AIMD.[8] This scheme will be applied to several elementary bimolecular addition reactions: (A) $BH_3 + H_2O \rightarrow H_2O{\cdot}BH_3$; (B) $BF_3 + NH_3 \rightarrow FB_3{\cdot}NH_3$; (C) $SO_3 + NH_3 \rightarrow O_3S{\cdot}NH_3$; (D) $C_2H_4 + CCl_2 \rightarrow H_4C_2{\cdot}CCl_2$; (E) $Ni(NH_2)_2 + PH_3 \rightarrow (NH_2)_2Ni{\cdot}PH_3$; (F) $W(CO)_5 + CO \rightarrow W(CO)_6$. In the current investigation, the method is only used to optimize minima and transition states along a path defined by a fixed reaction coordinate. In later investigations, we shall allow the reaction coordinate to be optimal so as to represent a minimum free energy path.

We organized this account as follows: The second part briefly presents the theoretical aspects of our calculations, including the calculation of the free energy gradient, the thermodynamic integration, and the Hessian update scheme. The optimized geometries along a path with a fixed reaction coordinate and the free energy profiles for the chosen six reactions, as well as some discussions, are presented in the third part. The conclusions will be offered in the final part.

Methodology

Consider a chemical system composed of N atoms of mass m_i ($i = 1, \cdots, N$). Although one can use $3N$ Cartesian coordinates to describe the system and its evolution, it is usually easier to use a set of $3N - 6$ generalized internal coordinates, as well as the overall rotation and translation of the molecule. Further, chemical intuition would suggest that most of the time only a few degrees of freedom (reaction coordinates) are sufficient to describe the reaction path. Thus, it appears natural to split the generalized coordinates into two subsets corresponding to the active coordinates, denoted by $\xi = (\xi_1, \cdots, \xi_r)$ and the inactive coordinates, denoted by $q = (q_1, \cdots, q_n)$. It is assumed that the reaction path (composed of active coordinates) runs along the bottom of the valley connecting the transition states with the reactants/products. This means that, during the whole dynamic simulations, the system will always regularly oscillate around

* To whom correspondence should be addressed. E-mail: ziegler@ucalgary.ca.

10.1021/jp045943n CCC: $30.25
Published on Web 12/13/2004

the minimum and stay equilibrated in the directions of the inactive coordinates, perpendicular to the path. Therefore, the procedure for the geometry optimization could be divided into two parts: one is for the active coordinates and one for the inactive coordinates. On the basis of the principle of "walking up the valley",[9] the equilibrium geometry parameters corresponding to the inactive coordinates could be obtained by averaging their values during the dynamic simulation.

$$q_i = \langle q_i \rangle_{\xi^*} \tag{1}$$

Here, ξ^* represents the active coordinates at fixed values and the brackets indicate an ensemble average of the system at the constraint values ξ^*.

For the active coordinate, we first have to calculate the derivative of the free energy and then use the same optimization scheme as that on the PES to find the stationary points. In this study, we will focus on the cases with one active coordinate corresponding to a fixed reaction coordinate. Recently, Fleurat-Lessard[8] has shown that the free energy gradient along a reaction coordinate can be calculated during AIMD simulations using the usual formulas:[10−13]

$$\left.\frac{\partial A(\xi)}{\partial \xi}\right)_{\xi^*} = \frac{1}{\langle |Z_\xi|^{-1/2} \rangle_{\xi^*}} \left\langle Z_\xi^{-1/2} \left(\lambda_\xi + \frac{1}{2\beta Z_\xi^2} \left\{ \sum_{i=1}^{3N} \frac{1}{m_i} \frac{\partial \xi}{\partial x_i} \frac{\partial Z_\xi}{\partial x_i} \right\} \right) \right\rangle_{\xi^*} \tag{2}$$

Here, β is Boltzmann's constant, ξ is the reaction coordinate, λ_ξ is the Lagrange multiplier associated with the reaction coordinate, which is the opposite of the force acting on the reaction coordinate, and Z_ξ is the part of the inverse mass matrix[8] corresponding to ξ:

$$Z_\xi = \sum_{i=1}^{3N} \frac{1}{m} \frac{\partial \xi}{\partial x_i} \frac{\partial \xi}{\partial x_i}$$

In some cases, such as the one in which ξ is a bond distance (as in the cases studied here) and Z_ξ is a constant, then eq 2 can be simplified to

$$\left.\frac{\partial A(\xi)}{\partial \xi}\right)_{\xi^*} = \langle \lambda_\xi \rangle_{\xi^*} \tag{3}$$

Once the derivative of the free energy has been evaluated, we can carry out the geometry optimization, as well as the calculation of the free energy change along the reaction coordinate.

Optimization of Stationary Points. The standard quasi-Newton method,[14−16] that uses gradients to update an approximate Hessian, was used to locate the stationary point in the direction of the fixed reaction coordination ξ. For the Hessian update, many methods can be used. Here, we adopted the Bofill[17] Hessian update scheme that is a combination of the Powell-symmetric-Broyden (PSB) and symmetric rank 1 (Murtagh-Sargent, MS)[14−16] update schemes.

$$\Delta H_{\text{Bofill}} = \phi \Delta H_{\text{MS}} + (1 - \phi) \Delta H_{\text{PSB}} \tag{4}$$

$$\phi = \frac{(\Delta x^t (\Delta g - H^{\text{old}} \Delta x))^2}{\Delta x^2 (\Delta g - H^{\text{old}} \Delta x)^2} \tag{5}$$

The rational function optimization (RFO) method[18] was used to control the Newton step in the optimization procedure.

Free Energy Change. Within a canonical (NVT) ensemble, the change in the Helmholtz free energy ΔA between two points, a and b, is given according to the thermodynamic integration method as

$$\Delta A_{a \to b} = \int_a^b \left\langle \frac{\partial A(\xi)}{\partial \xi} \right\rangle_\xi \mathrm{d}\xi = \int_a^b \langle \lambda_\xi \rangle_{\xi^*} \mathrm{d}\xi \tag{6}$$

The integral of eq 6 is typically evaluated through a finite difference numerical integration scheme referred to as pointwise thermodynamic integration (PTI).[19,20] In the PTI scheme, a small number of points along the reaction coordinate are chosen, and the system is allowed to dynamically evolve along all degrees perpendicular to the reaction coordinate. In this way, phase space is sampled at each point for a long time (3.4 ps) with no data collected between two points. The average force on the reaction coordinate at each point is then used as the ensemble average of the force in eq 6. One of the reviewers argued the convergence of the force. We adopted a much longer sampling time (16.8 ps), which just gave a force difference of less than 0.0005 Hartrees/Bohr. This indicates the sampling time at each point used here is sufficient.

Computational Details. A program, *FESOPT*, was used to carry out the geometry optimization. This program can automatically launch the AIMD simulation to get the gradient of the free energy and perform the quasi-Newton optimization procedure. The Car-Parrinello projected augmented wave (CP-PAW) program by Blöchl[6,7] was used for all AIMD simulations. The DFT functional used was that formed by the combination of the Perdew-Wang parametrization of the electron gas[21] in combination with the exchange gradient correction presented by Becke[22] and the correlation correction of Perdew.[23,24] Periodic boundary conditions were used, with a unit cell described by the lattice vectors ([0, 7.8, 7.8], [7.8, 0, 7.8], [7.8, 7.8, 0]) (Å) for all reactions. These unit cells were sufficiently large to ensure negligible overlap of the wave functions with the periodic images. In all calculations, the molecules have been electrostatically decoupled from their periodic images as described in ref 25. The energy cutoff used to define the basis set was 30 Ry (15 au) in all cases. The SHAKE algorithm[26] was used to impose constraints. The mass of hydrogen atoms was taken to be that of deuterium, and normal masses were taken for all other elements.

The CP-PAW calculations were performed at 0 K and at the two different target temperatures of 300 and 600 K. The Andersen thermostat[27] was applied to the nuclear motion by reassigning the velocity of N randomly chosen nuclei every n steps, where the values of N and n are chosen to maintain the desired temperature. In the cases of $BF_3 + NH_3$, $BH_3 + H_2O$, $SO_3 + NH_3$, and $C_2H_4 + CCl_2$, the reassignment was applied every 18 time steps. The reactions $Ni(NH_2)_2 + PH_3$ and $W(CO)_5 + CO$ used 2 reassignments for every 16 time steps. The thermostat settings were monitored and adjusted if necessary during the equilibration stage, with the main criteria for adequate thermostating being that the mean temperature was within a range of ±15 K and the temperature drift lower than 1.5 K/ps. In combination with the Andersen thermostat, a constant friction was applied to the wave function with a value of 0.003. For all reactions, a time step of 7 au was used.

In our dynamic simulations, another two constraints were applied to the system on top of the reaction coordinate. First, no translation of the center of mass of the whole system was allowed. Second, rotation of the total system about the center of mass was eliminated. Thus, to get the correct FES, the entropy contributions to the reaction free energy from the translation

and rotation of the whole system have to be added. We followed the correction scheme used by Kelly et al.[19] For a bimolecular reaction A + B → AB, the overall entropy correction from isolated reactants to a reaction coordinates (RC) of s is

$$\Delta S^{AB}_{PAWcorr}(s) = S^{AB}_{r}(s) + S^{AB}_{T}(s) - S^{A}_{T}(\infty) - S^{B}_{T}(\infty) \quad (7)$$

where $S^{AB}_{r}(s)$ is the rotational entropy at RC = s, which is geometry dependent, and $S^{AB}_{T}(s)$ is the translational entropy at RC = s. The last two terms represent the translational entropy of the isolated species A and B. The translational/rotational entropy terms to the right in eq 7 can be calculated easily from the translational/rotational partition functions.

Finally, the total free energy change $\Delta A^{AB}_{CM}(s)$ is obtained from a CP-PAW simulation with the constraints described here as

$$\Delta A^{AB}_{CM}(s) = \Delta A^{AB}_{PAW}(s) - T\Delta S^{AB}_{PAWcorr}(s) \quad (8)$$

where CM (classical mechanics) refers to the fact that the motion of the nuclei is described using classical mechanics. Further, $\Delta A^{AB}_{PAW}(s)$ is the change in free energy obtained directly from the simulation using eq 6.

It should be mentioned that the zero-point energy (ZPE) correction is not included in our simulations. This should not hamper our objective to perform a geometry optimization on the FES along a fixed reaction coordinate.

Results and Discussion

Differences between PES and FES. Before presenting our calculated results, we would like to give a qualitative analysis of the possible differences between the PES and FES.

As mentioned already, here, we work within a canonical (NVT) ensemble, and we get the Helmholtz free energy ΔA from the thermodynamic integration method. We have $\Delta A = \Delta U - T\Delta S$. Here, the first term ΔU is the internal energy that is composed of the electronic energy ΔE, the zero-point energy (ΔZPE, which is not included in our simulations as mentioned before), and the internal thermal energy ΔU_T (the contribution to the internal energy due to the heat capacities of the translational, electronic, rotational, and vibrational motions). Classically, $\Delta U_T = 0$[28] because each nuclear degree of freedom holds a constant energy of $^1/_2RT$, and the system is considered to remain in its electronic ground state. Hence, $\Delta U = \Delta E$ in our assumption. The second term $-T\Delta S$ is the entropy contribution.

For a bimolecular addition reaction A + B → AB of the type studied here, we define the distance (R) between A and B as the reaction coordinate. Thus, the PES is a curve of $\Delta E(R)$ versus R. For most cases, this curve is similar to a Morse potential curve without an energy barrier (see the PES in Figure 1). In some cases, however, the PES might have an energy maximum. If the entropy contribution ($-T\Delta S$) is added to the PES, we get the FES. It is clear that $\Delta S(R)$ increases with R, or in other words, $-T\Delta S(R)$ decreases with R. In a barrierless reaction, this decrease of the entropy (ΔS) is mostly due to the loss of translational and rotational motion of the fragments: as they come closer together, their relative motion turns into vibrations of the adduct, and the rotations of the fragments first become hindered and then split into one vibration and the overall rotation of the adduct. Here, we assume that $-T\Delta S(R)$ is a monotonically descending linear function for increasing values of R (see Figure 1).

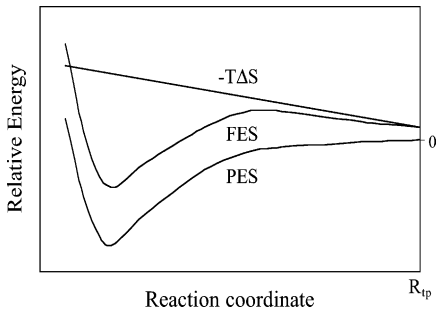

Figure 1. Schematic energy profiles of PES (ΔU), $-T\Delta S$, and FES ($\Delta A = \Delta U - T\Delta S$).

The whole process of the addition reaction A + B → AB can be thought to undergo two phases. The first phase corresponds to the approach of the two molecules from infinite distance to a "transition point" (R_{tp}), which is a critical point.[3] (When $R > R_{tp}$, the intermolecular interaction is negligible, whereas when $R < R_{tp}$, the two molecules start to react). An R_{tp} of 5.0 Å is used in this investigation. This was monitored by the criterion that the constraint force observed was, on average, close to zero for $R > 5.0$ Å. In this region ($R > 5.0$ Å), effectively no intermolecular interaction exists. The energy of the isolated species A and B was set to the energy zero point. Thus, at the point $R = 5.0$ Å, $\Delta U \approx 0$. However, the free energy is not zero, because the entropy is dependent on the intermolecular distance. Actually, the only contribution to ΔA at $R =$ 5.0 Å is $-T\Delta S$, due to the loss of transitional and rotational entropy, which can be easily obtained using eq 7.

The onset of the transition point ($R < R_{tp}$) is the second phase or the "reaction zone". In this region, the free energy has an ascending contribution due to the loss of entropy ($-T\Delta S$) and a descending contribution due to the intermolecular attraction. Different curvatures of the ascending ($-T\Delta S$) and descending (ΔU) curves will result in a different shape of the FES. Especially, a PES with a smaller curvature and a $-T\Delta S$ with a larger curvature will give rise to a free energy maximum on the FES (see Figure 1). We shall now discuss the individual reactions.

A. $BH_3 + H_2O \rightarrow H_3B{\cdot}OH_2$. The addition reaction of borane and water is very suitable for a more extensive test of the computational approaches due to its simplicity, although it is not of great interest experimentally. The PES and FES at 300 K have already been reported by our group.[19] Here, we will give the FES at 600 K, as well as the optimized geometries for the stationary points on the PES and FES at both 300 and 600 K along the fixed reaction coordinate.

The oxygen−boron intermolecular distance is chosen as the reaction coordinate. The PES and FES at 300 K (from ref 19) and 600 K are shown in Figure 2a. Here, one can see a typical Morse-type curve for the PES without any energy barrier. Starting at 4.5 Å, an obvious decrease in energy can be observed that indicates a significant dipole−quadrupole interaction between water and BH_3. The minimum in the PES corresponds to a binding energy of −14.2 kcal/mol (see Table 1), which is comparable with the binding energy of −14.9 kcal/mol by ADF[29] (TZP basis set) using the same functional. In the previous study of this reaction, the complexation energy was calculated at the G2 level and found to be −10.3 kcal/mol (including ZPE).[30] Let's now look at the FES at 300 K. Starting from the transition point (5.0 Å), the free energy increases first with decreasing B−O distance. At $R = 3.175$ Å, it reaches a free energy maximum (+3.2 kcal/mol, see Table 1). After that, the free energy decreases until it reaches the complexation product.

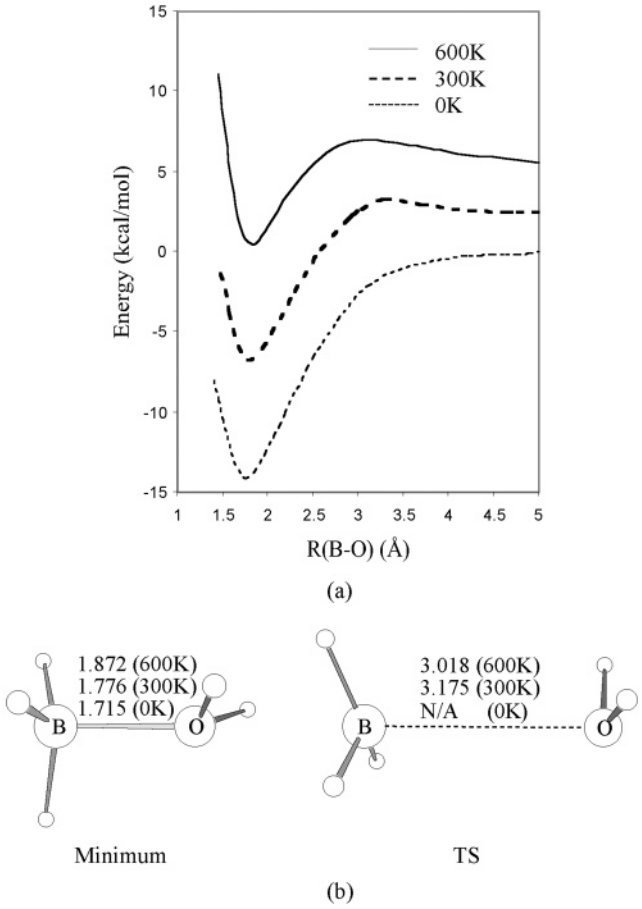

Figure 2. (a) Calculated potential energy profile and free energy profiles at 300 and 600 K along the reaction coordinate for the reaction $BH_3 + H_2O \rightarrow H_2O{\cdot}BH_3$. (Energy of the isolated species is set to 0). (b) Optimized values in the direction of the reaction coordinate for the complex and the transition state. Bond distances in Å.

TABLE 1: Calculated Complexation Energies and Possible Barriers along the Reaction Coordinate for Reactions A, B, C, D, E, and F[a]

	0 K	300 K	600 K
	barrier		
A. $BH_3 + H_2O$	N/A	+3.2	+7.0
B. $BF_3 + NH_3$	N/A	+3.5	+7.9
C. $SO_3 + NH_3$	N/A	N/A	+5.4
D. $C_2H_4 + CCl_2$	+1.4	+11.7	+18.9
E. $Ni(NH_2)_2 + PH_3$	+1.0	+5.8	+11.2
F. $W(CO)_5 + CO$	N/A	N/A	+4.3
	complexation energy		
A. $BH_3 + H_2O$	−14.2	−6.5	+0.5
B. $BF_3 + NH_3$	−16.7	−7.9	−0.4
C. $SO_3 + NH_3$	−17.6	−9.9	−2.3
D. $C_2H_4 + CCl_2$	−60.5	−45.8	−35.7
E. $Ni(NH_2)_2 + PH_3$	−16.5	−6.8	+1.5
F. $W(CO)_5 + CO$	−46.0	−38.1	−27.9

[a] Energies in kilocalories per mole. (N/A indicates no TS).

The complexation free energy at 300 K is −6.5 kcal/mol. For the FES at 600 K, there is also a free energy maximum that resides at $R = 3.018$ Å. The barrier (+7.0 kcal/mol) is 4 kcal/mol larger over that at 300 K.

Clearly, from the PES to the FES at 300 and 600 K, we can make the following observations: (1) There is no energy barrier on the PES, but there is one on the FES (both 300 and 600 K). This stems from the curvature difference between PES and $-T\Delta S$. (2) The TS shifts toward the product along the reaction coordinate when the temperature increases from 300 to 600 K. This is understandable, because the slope of $-T\Delta S$ increases with the temperature as a function of R. (3) The product shifts a little toward larger values of R as the temperature increases from 0 to 600 K, which can be attributed to the anharmonicity of the vibration motion. (4) The complexation energy decreases and the barrier increases with increasing temperature, which is due to the entropy contribution ($-T\Delta S$).

TABLE 2: Main Geometrical Parameters for the Minima and Transition States Optimized at 0, 300, and 600 K for the Reaction $BH_3 + H_2O \rightarrow H_2O{\cdot}BH_3$[a]

	0 K	300 K	600 K
	minimum		
B−O (Å)	1.715	1.776	1.872
B−H (Å)	1.219	1.221	1.222
O−H (Å)	0.984	0.987	0.989
H−B−H (°)	115.4	115.9	116.7
H−O−H (°)	106.6	106.9	106.7
	transition state		
B−O (Å)	N/A	3.175	3.018
B−H (Å)	N/A	1.208	1.219
O−H (Å)	N/A	0.985	0.988
H−B−H (°)	N/A	119.8	109.6
H−O−H (°)	N/A	104.2	104.3

[a] N/A indicates no TS.

The optimized structural parameters for the minima and transition states are shown in Table 2. For the minima, one can see that the bond distances increase a little with temperature. A relatively weak bond (like B−O) gives a larger change over the stronger bonds (B−H and O−H) with increasing temperature. This means that weak bonds have a much larger anharmonicity compared to the stronger bond. For the transition states, the bond distances corresponding to the inactive coordinates also elongate a little with temperature. However, the B−O distance, which is acting as the reaction coordinate, decreases from 3.175 Å at 300 K to 3.018 Å at 600 K. This contraction is due to the increase in the slope of $-T\Delta S$ with temperature.

B. $BF_3 + NH_3 \rightarrow F_3B{\cdot}NH_3$. As a typical model for a Lewis base/acid addition reaction, the process $BF_3 + NH_3 \rightarrow F_3B{\cdot}NH_3$ has been studied extensively. The B−N distance was chosen as the reaction coordinate. The calculated PES and FES at 300 and 600 K are shown in Figure 3a.

Again, a typical Morse-type curve without energy barriers was obtained for the PES. The complexation energy is −16.7 kcal/mol, which is 3 kcal/mol higher than the ADF/TZP result (−19.6 kcal/mol). The 3 kcal/mol energy difference probably originates from the limited projector functions. For the FES at 300 K, there is a free energy maximum (+3.5 kcal/mol) at $R = 3.440$ Å. The calculated complexation free energy ΔA at 300 K is −7.9 kcal/mol. The 600 K FES gives a much higher free energy barrier (+7.9 kcal/mol), and it resides at $R = 2.910$ Å. The calculated complexation energy is −0.4 kcal/mol. Clearly, the energy profiles obtained here are very similar to those obtained for the $BH_3 + H_2O$ system.

The important structural parameters for the optimized minimum and transition states are reported in Table 3. For the minima, one can see that the bond distances increase with temperature. It is found that stronger bonds give a smaller change with the increase of temperature. For the transition states, the bond distances corresponding to the inactive coordinates

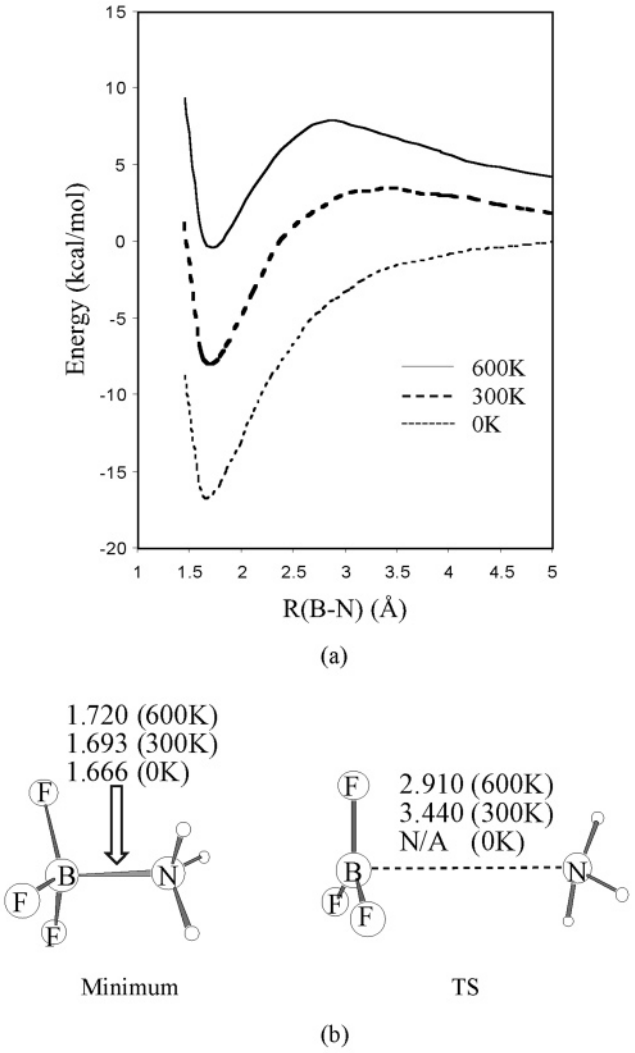

Figure 3. (a) Calculated potential energy profile and free energy profiles at 300 and 600 K along the reaction coordinate for the reaction $BF_3 + NH_3 \rightarrow BF_3{\cdot}NH_3$. (Energy of the isolated species is set to 0). (b) Optimized values in the direction of the reaction coordinate for the complex and the transition state. Bond distances in Å.

TABLE 3: Main Geometrical Parameters for the Minima and Transition States Optimized at 0, 300, and 600 K for the Reaction $BF_3 + NH_3 \rightarrow BF_3{\cdot}NH_3$[a]

	0 K	300 K	600 K
	minimum		
B−N (Å)	1.666	1.693	1.720
B−F (Å)	1.377	1.381	1.386
N−H (Å)	1.031	1.035	1.038
F−B−N (°)	104.1	104.5	104.3
H−N−B (°)	110.3	110.3	109.6
H−N−H (°)	108.6	108.4	108.4
F−B−F (°)	113.8	113.9	114.0
	transition state		
B−N (Å)	N/A	3.440	2.910
B−F (Å)	N/A	1.326	1.333
N−H (Å)	N/A	1.033	1.035
H−N−H (°)	N/A	106.6	107.3
F−B−F (°)	N/A	119.9	119.6

[a]N/A indicates no TS.

lengthen a little. A considerable change has been found for the B−N distance with temperature. It is shortened by about 0.5 Å when the temperature increases from 300 to 600 K.

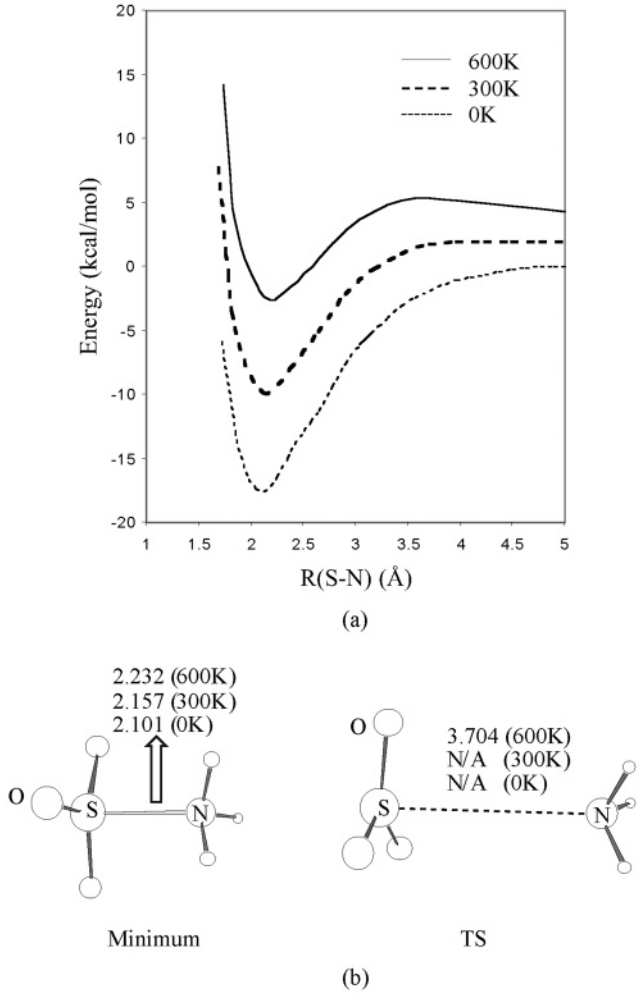

Figure 4. (a) Calculated potential energy profile and free energy profiles at 300 and 600 K along the reaction coordinate for the reaction $SO_3 + NH_3 \rightarrow O_3S{\cdot}NH_3$. (Energy of the isolated species is set to 0). (b) Optimized values in the direction of the reaction coordinate for the complex and the transition state. Bond distances in Å.

C. $SO_3 + NH_3 \rightarrow O_3S{\cdot}NH_3$. The results obtained for this reaction closely follow those obtained for reactions A and B. The calculated PES and FES at 300 and 600 K are shown in Figure 4a. The S−N distance was chosen as the reaction coordinate.

As for reactions A and B, a PES without a barrier is obtained for C. We calculated a complexation energy of −17.6 kcal/mol, which is comparable with −18.5 kcal/mol obtained with ADF/TZP. In contrast to reactions A and B, no free energy barrier could be found on the 300 K FES. The calculated complexation energy at 300 K is −9.9 kcal/mol. However, a transition state can be located on the 600 K FES with a barrier of +5.4 kcal/mol. The calculated complexation energy is −2.3 kcal/mol. This difference is understandable if we consider the difference in curvature of the PES between C and A/B. A much steeper PES for reaction C results in the term $-T\Delta S$ at a lower temperature failing to create a barrier.

The optimized structural parameters for the minima and transition states are shown in Table 4. For the minima, the trend for the bond distances to increase with temperature is found again.

D. $C_2H_4 + CCl_2 \rightarrow H_4C_2{\cdot}CCl_2$. The reaction of dichlorocarbene + ethene → 1,1-dichlorocyclopropane is a representative of the addition reaction between a carbene and an alkene. Previous studies have concentrated on the reaction mech-

TABLE 4: Main Geometrical Parameters for the Minima and Transition States Optimized at 0, 300, and 600 K for the Reaction $SO_3 + NH_3 \rightarrow O_3S{\cdot}NH_3$[a]

	0 K	300 K	600 K
	minimum		
S−N (Å)	2.101	2.157	2.232
S−O (Å)	1.453	1.455	1.457
N−H (Å)	1.030	1.033	1.036
O−S−N (°)	97.1	96.6	95.9
H−N−S (°)	108.7	108.5	107.9
H−N−H (°)	110.2	110.0	110.1
F−B−F (°)	118.4	118.6	118.7
	transition state		
S−N (Å)	N/A	N/A	3.704
S−O (Å)	N/A	N/A	1.455
N−H (Å)	N/A	N/A	1.037
H−N−H (°)	N/A	N/A	106.9
O−S−O (°)	N/A	N/A	119.4

[a] N/A indicates no TS.

anism.[31−36] It follows from these investigations that the addition reaction is a stepwise process: The first phase corresponds to an electrophilic addition of the carbene to one of the carbons constituting the double bond. The second phase is a nucleophilic attack on the second carbon of the double bond to close the cycle. Recently, this reaction has also been studied in our group in connection with the test of a new thermostate[19] and the development of a new method that can trace the minimum free energy path.[8] Here, we focus on the changes in stationary points and the energy profile on the FES at 300 and 600 K. The distance between the center of the double bond and the carbon of the carbene is chosen as the reaction coordinate. The calculated potential energy profile and free energy profiles at 300 and 600 K are shown in Figure 5a. (The energy profiles in Figure 5 correspond to the whole reaction process between the C_2H_4 and CCl_2, which involves both the first and second phases).

From the PES in Figure 5a, one finds a small energy barrier (+1.4 kcal/mol) and a very deep well-depth of −60.5 kcal/mol in energy. The FES at 300 K gives a higher barrier (+11.7 kcal/mol) and less deep well-depth (−45.8 kcal/mol). Further, a much higher barrier (+18.9 kcal/mol) and even less deep well-depth (−35.7 kcal/mol) are obtained on the 600 K FES. Only small shifts of the TS and minimum with temperature along the reaction coordinate can be observed (see Figure 5b).

The detailed structural parameters for the minima and transition states are shown in Table 5. The bond distances of the minima change very little with temperature because of the strong bonding interaction in the cyclopropane product. In the transition states, the C_3-C_2 and C_3-C_1 bond distances are shortened with the temperature increase, again due to the entropy contribution. The bond distances corresponding to the inactive coordinates elongate a little with the increase in temperature because of the anharmonicity.

E. $Ni(NH_2)_2 + PH_3 \rightarrow (NH_2)_2Ni{\cdot}PH_3$. The reaction of phosphine coordinating to a nickel center is another type of addition reaction. The Ni−P distance is taken as the reaction coordinate. The calculated PES and FES at 300 and 600 K are shown in Figure 6a.

As was the case in reaction D, there is a small barrier (+1.0 kcal/mol) on the PES. The calculated complexation energy is −16.5 kcal/mol, which is a little bit lower than the corresponding result of ADF/TZP (−14.8 kcal/mol). On the 300 K FES, a higher barrier (+5.8 kcal/mol) and a smaller binding energy (−6.8 kcal/mol) are obtained. And, the 600 K FES gives a much higher barrier (+11.2 kcal/mol) and a positive complexation energy of +1.5 kcal/mol.

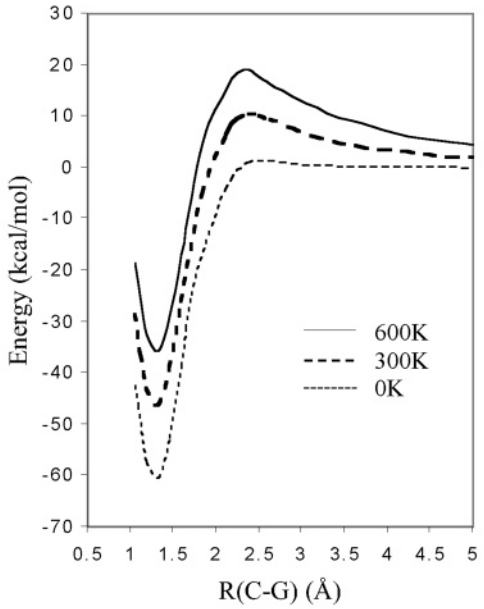

(a)

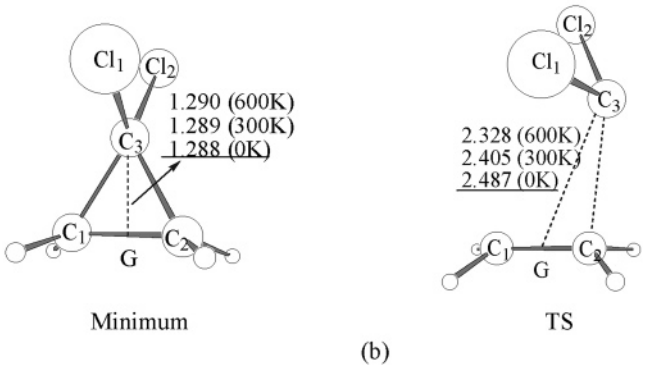

(b)

Figure 5. (a) Calculated potential energy profile and free energy profiles at 300 and 600 K along the reaction coordinate for the reaction $C_2H_4 + CCl_2 \rightarrow C_2H_4{\cdot}CCl_2$. (Energy of the isolated species is set to 0). (b) Optimized values in the direction of the reaction coordinate for the complex and the transition state. Bond distances in Å.

TABLE 5: Main Geometrical Parameters for the Minima and Transition States Optimized at 0, 300, and 600 K for the Reaction $C_2H_4 + CCl_2 \rightarrow C_2H_4{\cdot}CCl_2$.

	0 K	300 K	600 K
	minimum		
C_3-C_2 (Å)	1.497	1.502	1.503
C_3-C_1 (Å)	1.497	1.502	1.503
C_1-C_2 (Å)	1.527	1.532	1.538
C_3-Cl_l (Å)	1.777	1.782	1.784
$C_1-C_3-C_2$ (°)	62.3	61.3	61.5
	transition state		
C_3-C_2 (Å)	2.268	2.201	2.183
C_3-C_1 (Å)	2.855	2.765	2.729
C_1-C_2 (Å)	1.356	1.366	1.373
C_3-Cl_l (Å)	1.762	1.775	1.793
$C_1-C_3-C_2$ (°)	27.8	29.2	29.9

The detailed structural parameters for the minima and transition states are shown in Table 6. Clearly, the bond distances for the minima increase with temperature. The same trend has been found for the bond distances corresponding tothe inactive coordinates. The only exception is the Ni−P bond

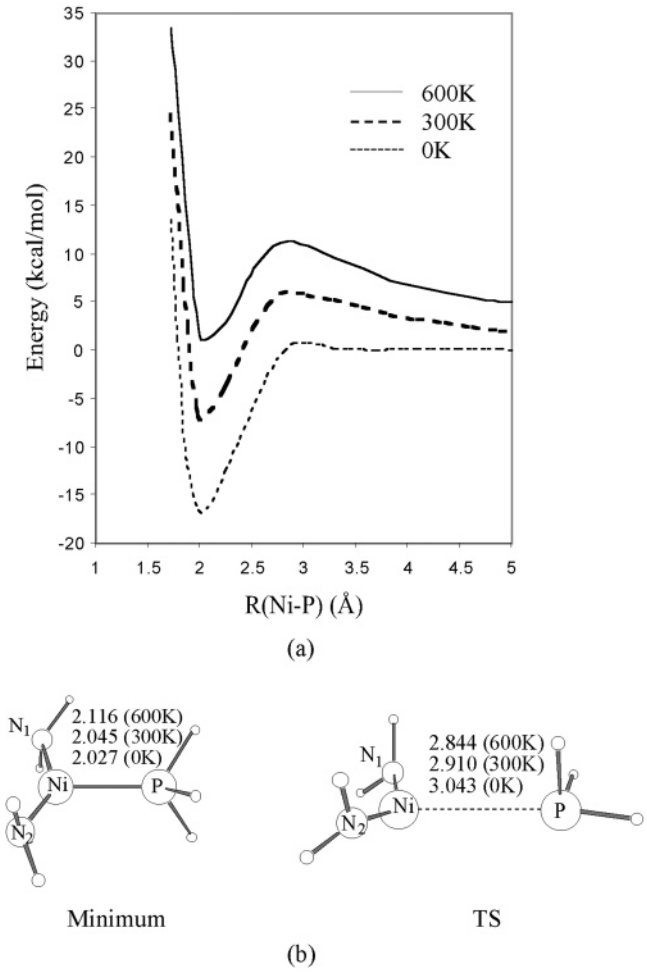

Figure 6. (a) Calculated potential energy profile and free energy profiles at 300 and 600 K along the reaction coordinate for the reaction $Ni(NH_2)_2 + PH_3 \rightarrow (NH_2)_2Ni{\cdot}PH_3$. (Energy of the isolated species is set to 0). (b) Optimized values in the direction of the reaction coordinate for the complex and the transition state. Bond distances in Å.

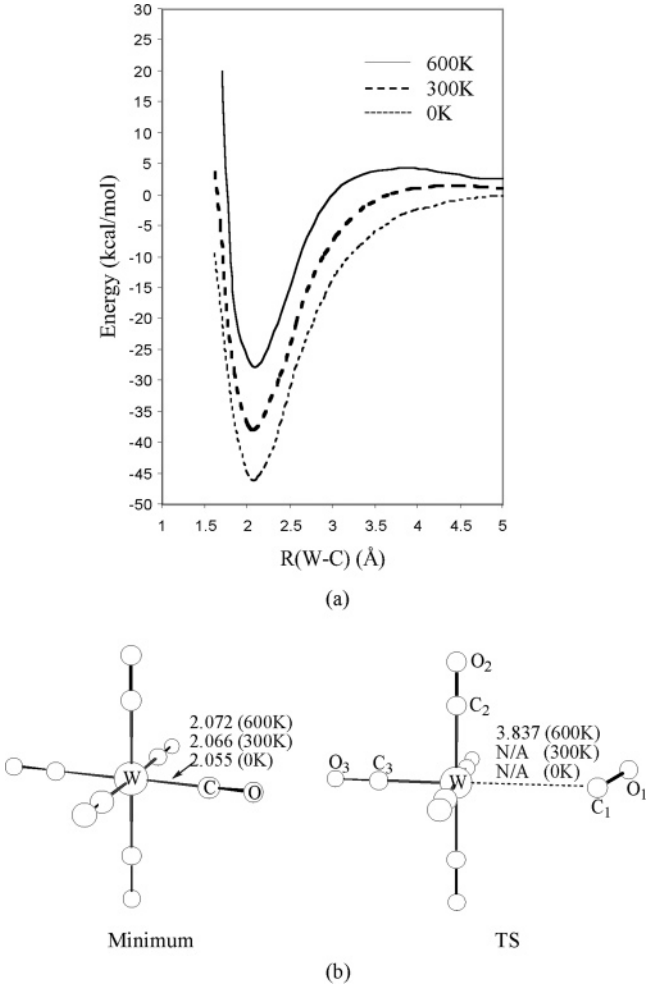

Figure 7. (a) Calculated potential energy profile and free energy profiles at 300and 600 K along the reaction coordinate for the reaction $W(CO)_5 + CO \rightarrow W(CO)_6$. (Energy of the isolated species is set to 0). (b) Optimized values in the direction of the reaction coordinate for the complex and the transition state. Bond distances in Å.

TABLE 6: Main Geometrical Parameters for the Minima and Transition States Optimized at 0, 300, and 600 K for the Reaction $Ni(NH_2)_2 + PH_3 \rightarrow (NH_2)_2Ni{\cdot}PH_3$

	0 K	300 K	600 K
		minimum	
Ni−P (Å)	2.027	2.045	2.116
Ni−N_1 (Å)	1.828	1.829	1.836
Ni−N_2 (Å)	1.813	1.825	1.830
N_1−Ni−P (°)	100.8	104.9	114.1
N_2−Ni−P (°)	110.2	106.0	114.7
		transition state	
Ni−P (Å)	3.043	2.910	2.844
Ni−N_1 (Å)	1.751	1.766	1.779
Ni−N_2 (Å)	1.749	1.763	1.774
N_1−Ni−P (°)	110.5	105.5	104.6
N_2−Ni−P (°)	102.0	110.7	110.4

distance, which is the reaction coordinate. It decreases with the temperature because of the increase in the slope of $-T\Delta S$.

F. $W(CO)_5 + CO \rightarrow W(CO)_6$. Transition-metal carbonyl complexes have been studied extensively. The chemical bonding between a transition metal and a CO ligand in carbonyl complexes is usually described in terms of donor−acceptor interactions between the occupied orbitals of the ligand and the empty orbitals of the metal, and vice versa.[37] Here, we have chosen a tungsten carbonyl complex as our model: the $W(CO)_5$ fragment complexes with CO. The W−C distance was chosen as the reaction coordinate. The calculated PES and FES at 300 and 600 K are shown in Figure 7a.

A barrierless PES has been obtained. The calculated complexation energy is −46.0 kcal/mol, which has a difference of only 2.1 kcal/mol compared with the ADF/TZP result (−48.1 kcal/mol). On the FES at 300 K, the complexation energy is −38.1 kcal/mol, and no barrier is obtained. However, on the 600 K FES, there is a TS with a barrier of +4.3 kcal/mol. The calculated complexation energy is −27.9 kcal/mol.

The detailed structural parameters for the minima and transition states are shown in Table 7. Again, the bond distances in the minima increase with the temperature.

Concluding Remarks

A scheme[8] for optimizing the structures of the minimum and the transition state on a free energy path along a fixed reaction coordinate has been applied here with the aid of ab initio molecular dynamics (AIMD). In the direction of the reaction coordinate, the values corresponding to the stationary points were optimized using a quasi-Newton method, in which the gradient of the free energy along the reaction coordinate was obtained by a constraint AIMD method. The Hessian was updated by the method of Bofill. The equilibrium values for

TABLE 7: Main Geometrical Parameters for the Minima and Transition States Optimized at 0, 300, and 600 K for the Reaction $W(CO)_5 + CO \rightarrow W(CO)_6$[a]

	0 K	300 K	600 K
	minima		
W−C (Å)	2.055	2.066	2.072
C−O (Å)	1.158	1.160	1.161
	transition state		
$W-C_1$ (Å)	N/A	N/A	3.837
$W-C_2$ (Å)	N/A	N/A	2.062
$W-C_3$ (Å)	N/A	N/A	1.946
$C1-O_1$ (Å)	N/A	N/A	1.146
$C2-O_2$ (Å)	N/A	N/A	1.163
$C3-O_3$ (Å)	N/A	N/A	1.172

[a] N/A indicates no TS.

the other directions were taken as the corresponding averages in the dynamic simulation.

The optimization scheme was applied to six bimolecular addition reactions: (A) $BH_3 + H_2O \rightarrow H_2O{\cdot}BH_3$; (B) $BF_3 + NH_3 \rightarrow FB_3{\cdot}NH_3$; (C) $SO_3 + NH_3 \rightarrow O_3S{\cdot}NH_3$; (D) $C_2H_4 + CCl_2 \rightarrow H_4C_2{\cdot}CCl_2$; (E) $Ni(NH_2)_2 + PH_3 \rightarrow (NH_2)_2Ni{\cdot}PH_3$; (F) $W(CO)_5 + CO \rightarrow W(CO)_6$. The optimized geometries for the minima and possible TS, for both the PES and the FES along the reaction coordinate, have been obtained. The main conclusions of this study can be summarized as follows:

(1) Different curvatures of ΔU and $-T\Delta S$ result in different shapes of the free energy profile. A barrierless PES with a smaller change rate of the potential energy in the reaction zone affords a barrier on the FES even at lower temperature, such as in reactions A and B studied here. A rapidly descending PES results in a barrier on the FES only at higher temperatures (600 K), like reactions C and F.

(2) On the FES, the barrier increases and the complexation energy decreases with temperature for the reactions studied here. This is due to the entropy contribution.

(3) With an increase in temperature, an obvious shift of the TS toward the complexation product, as well as a small shift of the minima toward the TS, have been observed. The TS shift could be attributed to the slope increase of the entropy contribution ($-T\Delta S$) with temperature. The minima shift is due to the anharmonicity of the bond vibration.

(4) It was observed that the bond distances corresponding to the inactive coordinates always increase with the temperature, which is due to thermal excitations and anharmonicity.

Acknowledgment. We thank Dr. Michael Seth for helpful discussions. This work was supported by the National Sciences and Engineering Research Council of Canada (NSERC). Calculations were performed in part on the Westgrid cluster and the MACI Alpha cluster located at the University of Calgary. T.Z. thanks the Canadian government for a Canada Research Chair. I.H. wishes to thank the Alberta Ingenuity Fund for their support.

References and Notes

(1) Ensing, B.; Laio, A.; Gervasio, F. L.; Parrinello, M.; Klein, M. L. *J. Am. Chem. Soc.* **2004**, *126*, 9492.
(2) Ammal, S. C.; Yamataka, H.; Aida, M.; Dupuis, M. *Science* **2003**, *299*, 1555.
(3) Yang, S.-Y.; Fleurat-Lessard, P.; Hristov, I.; Ziegler, T. *J. Phys. Chem. A* **2004**, *108*, 9461.
(4) Fletcher, R. *Practical Methods of Optimization*; John Wiley & Sons: New York, 1980. (b) Clark, T. *A Handbook of Computational Chemistry*; John Wiley & Sons: New York, 1985. (c) Jensen, F. *Introduction to Computational Chemistry*; John Wiley & Sons: New York, 1998.
(5) Pippard, A. B. *The Elements of Classical Thermodynamics*; Cambridge University Press: Cambridge, 1957. (b) Haile, J. *Molecular Dynamics Simulations*; John Wiley & Sons: New York, 1992. (c) Frenkel D.; Smit B. *Understanding Molecular Simulation*; Academic: San Diego, CA, 1996.
(6) Blöchl, P. E. *Phys. Rev. B* **1994**, *50*, 17953.
(7) Blöchl, P. E. *J. Phys. Chem.* **1995**, *99*, 7422.
(8) Fleurat-Lessard, P.; Ziegler, T. *J. Chem. Phys.*, in preparation.
(9) Here, "walking up the valley" means that a reaction path goes along the bottom of a valley connecting TS and the reactions/products in the direction perpendicular to the reaction coordinate.
(10) Den Otter, W. K.; Briels W. J. *J. Chem. Phys.* **1998**, *109*, 4139. (b) Den Otter, W. K.; Briels, W. J. *Mol. Phys.* **2000**, *98*, 773.
(11) Schlitter, J.; Klähn, M. *Mol. Phys.* **2003**, *101*, 3439.
(12) Sprik, M.; Ciccotti, G. *J. Chem. Phys.* **1998**, *109*, 7737.
(13) Darve, E.; Pohorille, A. *J. Chem. Phys.* **2001**, *115*, 9169. (b) Darve, E.; Pohorille, A. *Mol. Simul.* **2002**, *28*, 113.
(14) Dennis, J. E.; Schnabel, R. B. *Numerical Methods for Unconstrained Optimization and Nonlinear Equations*; Prentice Hall: Englewood Cliffs, NJ, 1983.
(15) Scales, L. E. *Introduction to Non-Linear Optimization*; Springer-Verlag: New York, 1985.
(16) Gill, P. E.; Murray, W.; Wright, M. H. *Practical Optimization*; Academic Press: London, 1981.
(17) Bofill, J. M. *J. Comput. Chem.* **1994**, *15*, 1.
(18) Banerjee, A.; Adams, N.; Simons, J.; Shepard, R. *J. Phys. Chem.* **1985**, *89*, 52.
(19) Kelly, E.; Seth, M.; Ziegler, T. *J. Phys. Chem. A* **2004**, *108*, 2167.
(20) Straatsma, T. P.; McCammon, J. A. *J. Chem. Phys.* **1991**, *95*, 1175.
(21) Perdew, J. P.; Wang, Y. *Phys. Rev. B* **1992**, *45*, 13244.
(22) Becke, A. *Phys. Rev. A* **1988**, *38*, 3098.
(23) Perdew, J. P. *Phys. Rev. B* **1986**, *34*, 7406.
(24) Perdew, J. P. *Phys. Rev. B* **1986**, *33*, 8822.
(25) Blöchl, P. E. *J. Chem. Phys.* **1995**, *103*, 7422.
(26) Ryckaert, J. P.; Cicotti, G.; Berensden, H. J. *J. Comput. Phys.* **1977**, *23*, 327.
(27) Andersen, H. C. *J. Chem. Phys.* **1980**, *72*, 2384.
(28) McQuarrie, D. A. *Statistical Thermodynamics*; Harper and Row: New York, 1973.
(29) Baerends, E. J.; Ellis, D. E.; Ros, P. *Chem. Phys.* **1973**, *2*, 41. (b) Baerends, E. J.; Ros, P. *Chem. Phys.* **1973**, *2*, 52. (c) te Velde, G.; Baerends, E. J. *J. Comput. Phys.* **1992**, *92*, 84. (d) Fonseca, C. G.; Visser, O.; Snijders, J. G.; te Velde, G.; Baerends, E. J. In *Methods and Techniques in Computational Chemistry*, METECC-95; Clementi, E., Corongiu, G., Eds.; STEF: Cagliari, Italy, 1995; p 305.
(30) Anane, H.; Boutalib, A.; Tomás, F. *J. Phys. Chem. A* **1997**, *101*, 7879.
(31) Rondan, N. G.; Houk, K. N.; Moss, R. A. *J. Am. Chem. Soc.* **1980**, *102*, 1770.
(32) Wong, P. C.; Griller, D.; Scaiano, J. L. *Chem. Phys. Lett.* **1981**, *103*, 2423.
(33) Turro, N. J.; Lehr, G. F.; Butcher, J. A.; Moss, R. A.; Guo, W. *J. Am. Chem. Soc.* **1982**, *104*, 1754.
(34) Moss, R. A.; Perez, L. A.; Turro, N. J.; Gould, I. R.; Hacker, N. P. *Tetrahedron Lett.* **1983**, *24*, 685.
(35) Houk, K. N.; Rondan, N. G.; Mareda, J. *J. Am. Chem. Soc.* **1984**, *106*, 4291.
(36) Blake, J. F.; Wierschke, S. G.; Jorgensen, W. L. *J. Am. Chem. Soc.* **1989**, *111*, 1119.
(37) Dewar, M. J. S. *Bull. Soc. Chim. Fr.* **1951**, *18*, C79.